Araştırma Makalesi
Adıyaman Üniversitesi Mühendislik Bilimleri Dergisi
16 (2022) 69-77

EFFECTS OF PH AND CURRENT DENSITY ON MICROSTRUCTURE AND HARDNESS OF THE COBALT-TUNGSTEN ALLOY

Kürşad Oğuz OSKAY*

Sivas Cumhuriyet Üniversity, Faculty of Engineering, Metallurgical and Materials Engineering, Sivas, 58040, Türkiye
Geliş Tarihi/Received Date: 10.10.2021 Kabul Tarihi/Accepted Date: 22.03.2022 DOI: 10.54365/adyumbd.1007722

ABSTRACT

In this study, cobalt-tungsten coatings were electrodeposited on copper substrates. Nanocrystalline and amorphous cobalt tungsten alloys were electrodeposited from citrate-boric acid baths. The characterization of the alloy coatings was carried out by scanning electron microscopy (SEM), X-ray fluorescence (XRF), and X-ray diffraction (XRD). The most significant factors, such as current density and pH of the electrolyte that affect the morphology, tungsten composition, and microhardness value, were studied. The tungsten content of the electrodeposits varied 11 to 46% by changing process variables. The microhardness value of the coatings was decreased dramatically when the tungsten composition exceeded 35%. Response surface methodology was used to construct models for predicting microhardness value and tungsten composition of the coating. The optimal conditions for the electrodeposition were found as follows: current density of 5A/dm2 and pH 6. Under optimal conditions, the coating exhibits a hardness of 570 HV.

Keywords: *Cobalt, tungsten, electrodeposition*

PH VE AKIM YOĞUNLUĞUNUN KOBALT-TUNGSTEN KAPLAMALARININ MIKROYAPI VE SERTLIĞINE ETKILERI

ÖZET

Bu çalışmada, bakır altlık malzemeler kullanılarak kobalt tungsten kaplamalar üretilmiştir. Sitrat-borat banyosu kullanılarak yapılan çalışmalarda, nanokristalin ve amorf kobalt-tungsten kaplamalar üretilmiştir. Kaplamaların karakterizasyonu için taramalı elektron mikroskobu (SEM), X-ışını floresansı (XRF) ve X-ışını kırınımı (XRD) cihazları kullanılmıştır. pH ve akım yoğunluğunun, kaplama morfolojisine, tungsten bileşimine ve mikrosertlik değerine etkileri incelenmiştir. Çalışmalar sırasında proses değişkenleri değiştirilerek üretilen numunelerin tungsten içeriği %11 ile 46 arasında değişmiştir. Deneylerde en yüksek sertlik değeri olarak 570 HV ölçülmüştür. Elektrolit pH'ı 6 olarak seçilen bu deneyde uygulanan akım yoğunluğu ise 5A/dm2'dir. Kaplamaların tungsten içeriğinin %35'i geçmesi ile kaplamaların sertliklerinde düşüş gözlemlenmiştir. Cevap yüzey yöntemi kullanılarak kaplamanın mikrosertlik değeri ve tungsten bileşimini tahmin edebilecek matematiksel modeller oluşturulmuştur.

Anahtar Kelimeler: *Kobalt,tungsten, elektrokaplama*

1. Introduction

Its outstanding properties and numerous potential applications have propelled the interest in tungsten and its alloys. These alloys can be prepared using various methods [1, 2]. In order to prepare these coatings, one option is to use electrodeposition, which has obvious advantages such as simplicity, uniformity, low cost, and scalability, in comparison with the other coating methods. Electrodeposition is a versatile and cost-effective method for fabricating a wide variety of two and three-dimensional coatings. In this process, dissolved metal cations are reduced employing an electric current, resulting in a thin, coherent metal coating on an electrode. Unfortunately, tungsten cannot be deposited from an

* e-posta: kursadoskay@gmail.com ORCID ID: https://orcid.org/0000-0003-4026-867X (Sorumlu Yazar),

aqueous solution as a pure metal unless it can be co-deposited with iron group metals as an alloy. This type of electrodeposition is known as induced electrodeposition [3]. The interest in electrodeposited tungsten alloys with iron-group metals has increased in recent years due to their unique combination of anticorrosive [4], magnetic [5], and catalytic properties [6]. In addition, Co–W coatings are regarded as a suitable material for the defence industry, instead of hard chromium coatings deposited using hazardous hexavalent chromium baths [7, 8].

Plating bath composition and deposition parameters influence tungsten-containing alloy coating composition and microstructure [9]. The electrodeposition of Co-W alloys is reported from various electrolytes such as gluconate [10, 11], citrate-borate [12, 13], citrate-ammonia [14]. Citrate is one of the most commonly used additives in electrodeposition because it is a powerful complexing agent for a wide range of metals, including cobalt, nickel, copper, and tungsten. Besides, the citrate borate bath is environmentally friendly [15].

Electrolyte pH has a significant effect on the composition of alloy coating, deposition rate, and hardness. Because the formation of complexed cobalt-tungstate-citrate species is pH-dependent.

Due to the hydrogen evolution, pH increases near the electrode, and ammonia or ammonium salts can be used for buffering purposes. Electrodeposition of metal alloys from aqueous baths generally is carried out in non-hermetic cells [16]. In this situation, a considerable amount of ammonia can evaporate during long-term electrodeposition at higher temperatures. As a result, non-volatile citrate electrolytes using boric acid as a buffering agent rather than ammonia are preferable for long-term electrodeposition at elevated temperatures [16]. Because of this reason citrate-borate bath was used in this study.

To the best of our knowledge, there are no previous literature reports about optimising the Co-W electrodeposition process by central composite design method. Thus, this study is aimed to make the Co-W electrodeposition process commercially more viable by understanding the dominant process parameters that affect the coating microstructure and specifications by constructing mathematical models. For this purpose, the tungsten composition and microhardness value of the coating was selected as the responses. The pH and current density were selected as the factors that affects the responses.

2. Materials and Methods

Co-W coating was prepared by using a citrate-borate bath. Distilled water and analytical grade chemicals were used to prepare the plating solution. Table 1. shows the plating solution concentration and operational parameters. In addition, citric acid, sodium citrate dehydrate, and boric acid concentrations are held constant and listed in Table 1.

A platinized titanium net with dimensions of 250x300x100mm was used as an anode, and a copper plate was used as the cathode. Pretreatment of the working surface prior to the plating process includes ultrasonic cleaning in an organic solvent, water rinsing, anodic etching in phosphoric acid (80%) for 5 minutes at 1.5V. Then cathode was immersed in 10% HNO_3 and 1% H_2SO_4 solution for 1 minute respectively and rinsed in distilled water to remove oxides from the surface.

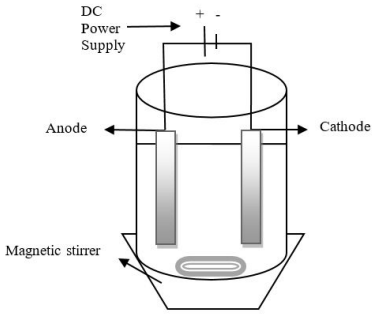

Figure 1. Schematic representation of electrodeposition cell.

All the coatings were fabricated using the DC electrodeposition method with a deposition time of 180 min at 60 °C. The electrolyte pH was maintained at 6, 7 and 8, which was adjusted by adding sulphuric acid or sodium hydroxide when necessary. As shown in Figure 1, the electrodeposition experiments were carried out in a beaker. The bath was stirred and heated by a magnetic stirrer.

Table 1. Plating bath compositions and operational parameters.

Factor	**-1**	**0**	**1**
(X1) Electrolyte pH	6	7	8
(X2) Current Density (A/cm^2)	5	7.5	10
Constant Parameters			
Plating temperature :	60 °C	$C_6H_8O_7$:	7g/L
$CoSO_4.6H_2O$	60g/L	$Na_3C_6H_5O_7.2H_2O$(M):	15g/L
Na_2WO_4	15g/L	H_3BO_3:	40g/L

The microstructure of the samples was characterized by field emission gun scanning electron microscopy (FE-SEM, Tescan Mira3 XMU, Czech Republic), following phase constituent analysis using (XRD, Bruker AXS D8 Advance, Germany). The chemical composition of the coatings was characterized by X-ray fluorescence (XRF, Niton XL3T, USA). The microhardness of the coatings was measured by the Vickers hardness (Shimadzu MHV tester) method, and the mean of at least five readings was taken.

3. Results and Discussion

3.1. Design of Experiments

The experimental studies in this research were carried out using a Central Composite Design (CCD), which is a widely used form of Response Surface Methodology (RSM). Factors and levels that are used in CCD are presented in Table 1. CCD experiment results and the predicted values were given in Table 2. The predicted results obtained via mathematical models and experiments were consistent with each other. Equations were given in Table 3 and 4, where R_w and R_m are the tungsten composition and microhardness value of the coating, respectively. The analysis of variance (ANOVA) and the F- test were used to estimate the model's significance. The ANOVA of the regression models, shown in Tables 3 and 4, shows that the models are highly significant, as evidenced by the derived F-values for tungsten composition and microhardness value, which are 93.98 and 18.47, respectively. It was revealed that the models employed to fit the response variables were significant and appropriate in terms of expressing the relationship between the response and independent variables, according to the results. [17]. The response surface graphs that define tungsten composition and microhardness of the coating with the data obtained from mathematical models were given in Figure 2.

Table 2. Design of experiments, experimental and predicted results.

			Experimental Results		**Predicted Results**	
Run	**pH**	**Current Density (A/dm^2)**	**Tungsten Composition (%)**	**Microhardness (Hv)**	**Tungsten Composition (%)**	**Microhardness (Hv)**
1	6	5	15	570	14.67	550.28
2	8	7.5	42	354	43.00	270.11
3	6	7.5	11	530	11.67	528.78

4	8	5	45	245	44.50	291.61
5	7	7.5	40	320	38.33	399.44
6	8	10	46	235	45.50	248.61
7	6	10	13	510	12.67	507.28
8	7	10	45	386	45.83	377.94
9	7	5	34	445	34.83	420.94

Table 2. Continue

Table 3. ANOVA table of R_w (Tungsten composition of the coating)

Source	Sum of Squares	df	Mean Square	F-Value	p-value Prob > F
Model	1785.667	6	297.6111	93.98246	0.0106
A-Ph	1472.667	1	1472.667	465.0526	0.0021
B-Current Density	60.5	1	60.5	19.10526	0.0486
AB	2.25	1	2.25	0.710526	0.4880
A^2	242	1	242	76.42105	0.0128
B^2	8	1	8	2.526316	0.2529
A^2B	44.08333	1	44.08333	13.92105	0.0649
Residual	6.333333	2	3.166667		
Cor Total	1792	8			
R^2=0.996 R^2_{adj}=0.985					
R_w (%) =38.33+15.67*A+5.50*B+0.75*A*B-11.00*A^2+2.00*B^2-5.75*A^2 * B					

Table 4. ANOVA Table of R_m (Microhardness value of the coating)

Source	Sum of Squares	df	Mean Square	F-Value	p-value Prob > F
Model	103136.2	2	51568.08	18.47429	0.0027
A-Ph	100362.7	1	100362.7	35.95498	0.0010
B- Current Density	2773.5	1	2773.5	0.993608	0.3573
Residual	16748.06	6	2791.343		
Cor Total	119884.2	8			
R^2=0.861 R^2_{adj}=0.813					
R_m (Hv) =+399.44-129.33*A-21.50*B					

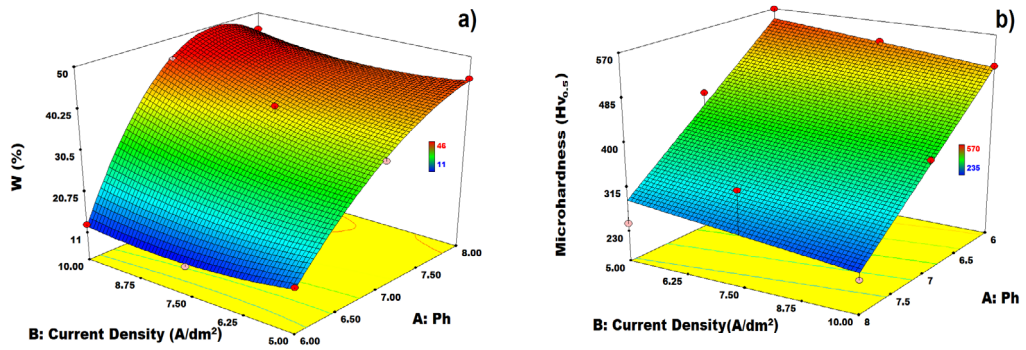

Figure 2. Response surface graphs obtained from the mathematical models a) Tungsten composition of the coating, b) Microhardness of the coating.

Figure. 2a and 2b show the effect of current density and pH on the composition of tungsten and microhardness value of the coating, respectively. As seen in the response surface plots, the pH value of the solution is the dominant factor for the electrodeposition of Co-W alloy.

The tungsten content of the deposit increases linearly with increasing pH of the electrolyte at acidic conditions, but the increment decreases slightly after the 7.5 pH value. Similar findings have been reported in the literature [18]. Tungsten reduction occurs more efficiently in the pH range due to the enhanced adsorption of electroreduced W containing complexes, increasing the tungsten content of Co–W alloys. [13].

The hardness of the Co-W alloy electrodeposit is determined by many factors such as composition, structure, and morphology. For the studied experimental condition, the tungsten content and microhardness value of the deposit slightly depend on the current density since the effect of the pH is dominant. It can be seen that the microhardness value of the coating was significantly enhanced at low current densities when examining Table 2. It is observed that the microhardness of the electrodeposit decreases linearly with decreasing pH. A possible explanation for this trend is that the electrodeposit contains tungsten in high concentrations. Similar studies were reported that with the increment of tungsten composition to a particular value, the microhardness value decreases dramatically [19]. In our study, when the tungsten level of the coatings exceeds 35%, the microhardness value declines significantly.

3.1. Surface and XRD Characterization

The SEM images of the alloy electrodeposit surface were presented in Figure 3. The tungsten composition of the electrodeposit can be altered over a broad range (11-46%) by simply adjusting the pH. Coatings deposited at pH 8 contain greater than 35% W, a bright, mirror-like coating with a metallic appearance rather than a gray appearance. An increase in current density at pH 6, leads to a transition towards more regular and elongated features on the morphology. On the other hand, with the increase of pH 7 to 8 the structure becomes more compact and consists of nodular-shaped grains. In addition, nodular grain size decreases with the increase of current density at pH 8. The rise in current density encourages cathodic depolarization, which in turn promotes the production of nuclei. This further reduces the size of the aggregate grains. Typical changes in the diffraction patterns of the amorphous and nanocrystalline Co-W coatings with different W content are shown in Figure 4. The XRD spectrums show that the crystallographic structure is changing from nanocrystalline to amorphous as the amount of the W increases. A broad peak was observed in the proximity of $2\theta = 44.4^{o}$. This peak broadening can be ascribed to the small crystallite size of the alloy that contains over 40% tungsten composition. [20]. Meanwhile, nanocrystalline peaks on the XRD pattern for the Run 6 experiment (Figure 4) suggest the incorporated Co(W) crystals in the amorphous matrix, which is consistent with the literature [21].

XRD patterns of Co-W alloys are illustrated in Figure 4. The nanocrystalline coating showed four peaks at 2θ values of 41.6, 44.7, 47.5, and 75.9. These peaks are related to hcp Co (JCPDS 05-0727). However, peak positions of hcp Co shifted to a lower 2θ value in Figure 4, which confirms the incorporation of tungsten cobalt crystal lattice [22]. From the XRD diagram in Figure 4, it is clear that current density affected their crystallographic orientation. With increasing current density, the reflection corresponding to Co (002) is disappeared, and sharp Co (100) reflection is observed.

In order to estimate the crystallite size Debye Scherrer equation was used. As seen in Figure 4. Run 6 consists of nanocrystalline (62^{o} and 76^{o}) and amorphous peaks (44^{o}). Calculations made by taking into account the (102) and (110) peaks, the crystallite size was calculated as 16 nm for Run 6 experiment. While ignoring these peaks, the crystallite size of the amorphous structure was calculated as 1.7 nm. The relations between crystallite size and microhardness can be clarified with the Hall–Petch relationship [16]. For example, electrodeposited coatings with crystallite sizes 30 and 38 nm (Run 1 and Run 7) properly obeys the Hall-Petch equation and microhardness increases with the decrease of crystallite size.

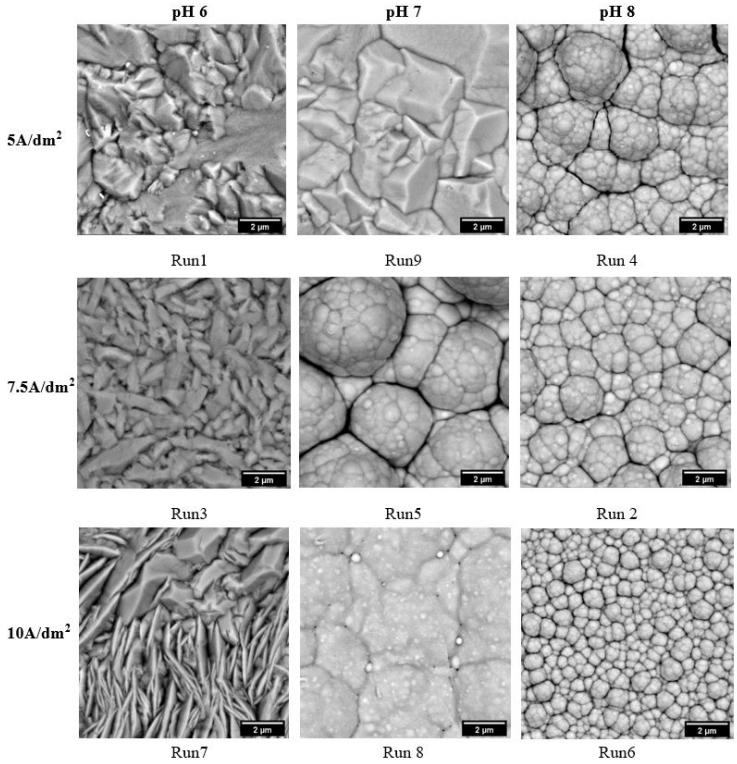

Figure 3. SEM images of Co-W alloys electrodeposited with various parameters.

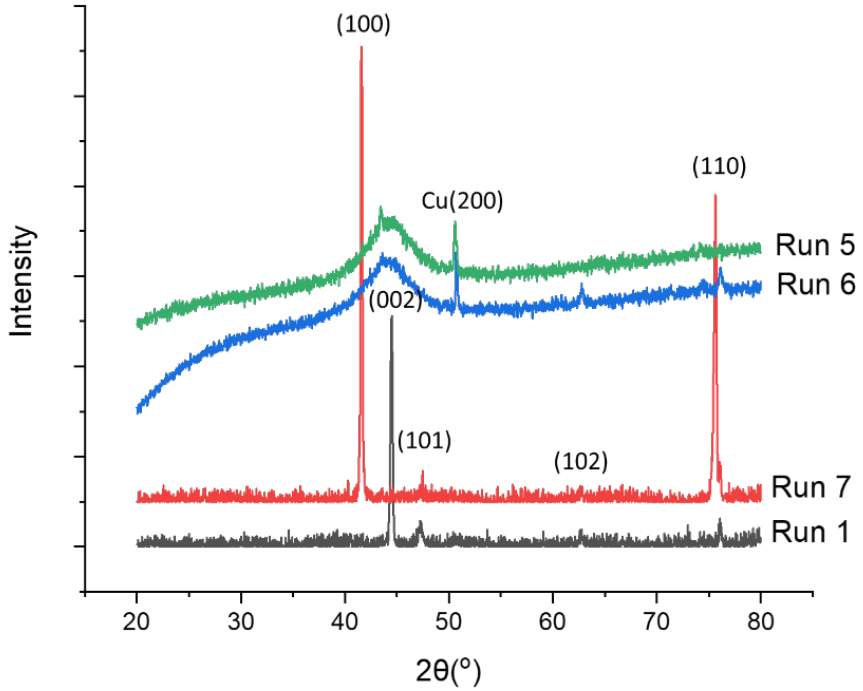

Figure 4. X-ray diffraction pattern of Run1, Run7, Run5 and Run6 samples.

Nanocrystalline coatings had a higher microhardness value despite the higher tungsten content in amorphous coating. Amorphous coatings with crystallite sizes 1.7 and 1.9 nm did not follow Hall-Petch,

and microhardness value was declined with the decrease of crystallite size [23]. Similar behaviours about microhardness value that depend on the crystallite size were reported by other researchers who worked with iron group metal-tungston alloys [7, 24, 25]. They reported that incorporation of W in Co up to ~20 wt-% causes a significant increase in the microhardness value. However, the larger incorporation of W decreases the microhardness value. The softening effect related to grain size reduction may be attributed to an increase in intercrystalline volume fraction, particularly the percentage associated with the triple junction. The deformation of the grain boundary volume considerably contributes to the overall deformation in such a microstructure. The grain boundaries of fine-grained material were thicker than those of coarse-grained material when the grain size was less than 10 nm. A critical Hall-Petch breakdown crystallite size of 12-15 nm for Ni-W electrodeposits was also reported by Wasekar et al. [26]. The interface region of the nanocrystallites having a structure of non-periodic atomic array expanded into the centre region [27]. Thus, the incorporation of tungsten over 35% adversely affected the microhardness for the reasons stated above.

Table 5. Microhardness value and Crystallite size calculations based on Debye Scherrer equation.

Tungsten Composition (%)	Crystallite size (nm)	Microhardness (HV)
13	30	570
15	38	510
40	1.9	320
46	1.7	235

4. Conclusion

In summary, based on the results of this study showed that the tungsten composition of the electrodeposit affects the microhardness and morphology of the coating. With the increment of the tungsten content of more than %35, amorphous behaviour was observed, and electrodeposit microhardness was decreased. Response surface methodology was used to construct a model that defines the microhardness value and tungsten composition of the electrodeposit. Predicted results calculated by models were in good accordance with experimental results. In other words, these results indicate that the constructed statistical models could effectively predict the tungsten composition and microhardness value of the coating.

Acknowledgements

("This work is supported by the Scientific Research Project Fund of Sivas Cumhuriyet University under the project number M-788")

References

[1] Su YH, Kuo TC, Lee WH et al. Effect of tungsten incorporation in cobalt tungsten alloys as seedless diffusion barrier materials. Microelectronic Engineering 2017; 171: 25–30.
[2] Fu T, Cui K, Zhang Y et al. Oxidation protection of tungsten alloys for nuclear fusion applications: A comprehensive review. J Alloys Compd 2021; 884: 161057.
[3] Belevskii SS, Gotelyak A V, Yushchenko SP, Dikusar AI. Electrodeposition of Nanocrystalline Fe − W Coatings from a Citrate Bath. Surface Engineering and Applied Electrochemistry 2019;

55: 119–129.
[4] Costa JM, Porto MB, Amancio RJ, de Almeida Neto AF. Effects of tungsten and cobalt concentration on microstructure and anticorrosive property of cobalt-tungsten alloys. Surfaces and Interfaces 2020; 20.
[5] Wei GY, Lou JW, Ge HL et al. Co-W films prepared from electroplating baths with different complexing agents. Surface Engineering 2012; 28: 412–417.
[6] Vernickaite E, Tsyntsaru N, Sobczak K, Cesiulis H. Electrodeposited tungsten-rich Ni-W, Co-W and Fe-W cathodes for efficient hydrogen evolution in alkaline medium. Electrochimica Acta 2019; 318: 597–606.
[7] Fathollahzade N, Raeissi K. Electrochemical evaluation of corrosion and tribocorrosion behaviour of amorphous and nanocrystalline cobalt-tungsten electrodeposited coatings. Materials Chemistry Physics 2014; 148: 67–76.
[8] Dadvand N, Jarjoura G, Kipouros GJ. Electrodeposition of cobalt-tungsten alloys from alkaline citrate containing bath as alternative for chromium hexavalent replacement. Canadian Metallurgical Quarterly 2013; 52: 391–397.
[9] Vernickaite E, Cesiulis H, Tsyntsaru N. Evaluation of corrosion and tribological behavior of electrodeposited tungsten alloys. Proc 9th Int Sci Conf BALTTRIB 2017 - Dedic to 100th Anniv Restit Lith 2018; 207–214.
[10] Belevskii SS, Bobanova JI, Buravets VA et al. The influence of gluconate bath parameters on the rate of electrodeposition and mechanical properties of Co–W coatings. Proc 9th Int Sci Conf BALTTRIB 2017 - Dedic to 100th Anniv Restit Lith 2018; 7–12.
[11] Weston DP, Harris SJ, Capel H et al. Nanostructured Co-W coatings produced by electrodeposition to replace hard Cr on aerospace components. The International Journal of Surface Engineering and Coatings 2010; 88: 47–56.
[12] Frank AC, Sumodjo PTA. Electrodeposition of cobalt from citrate containing baths. Electrochim Acta 2014; 132: 75–82.
[13] Tsyntsaru N, Cesiulis H, Budreika A et al. The effect of electrodeposition conditions and post-annealing on nanostructure of Co-W coatings. Surface Coatings Technology 2012; 206: 4262–4269.
[14] Bodaghi A, Hosseini J. Corrosion behavior of electrodeposited cobalt-tungsten alloy coatings in NaCl aqueous solution. International Journal of Electrochemical Science 2012; 7: 2584–2595.
[15] Frank AC, Sumodjo PTA. Electrodeposition of cobalt from citrate containing baths. Electrochimica Acta 2014; 132: 75–82.
[16] Tsyntsaru N, Cesiulis H, Donten M et al. Modern trends in tungsten alloys electrodeposition with iron group metals. Surface Engineering Applied Electrochemistry 2012; 48: 491–520.
[17] Oskay KO, Demirel B. Research Article Optimizing the composition of electroplated composite coating NiCrAl. Acta Physica Polonica A 2018; 36: 801–808.
[18] Ma L, Xi X, Nie Z, Dong T, Mao Y. Electrodeposition and characterization of Co-W Alloy from regenerated Tungsten salt. Int J Electrochem Sci 2017; 12: 1034–1051.
[19] Costa JD, de Sousa MB, Alves JJN et al. Effect of electrochemical bath composition on the preparation of Ni-W-Fe-P amorphous alloy. International Journal of Electrochemical Science 2018; 13: 2969–2985.
[20] Vernickaite E, Tsyntsaru N, Cesiulis H. Electrodeposited Co-W alloys and their prospects as effective anode for methanol oxidation in acidic media. Surface Coatings Technology 2016; 307: 1322–1328.
[21] Nicolenco A, Tsyntsaru N, Fornell J et al. Mapping of magnetic and mechanical properties of Fe-W alloys electrodeposited from Fe(III)-based glycolate-citrate bath. Mater Des 2018; 139: 429–438.
[22] Vernickaite E, Tsyntsaru N, Cesiulis H. Electrodeposition and corrosion behaviour of nanostructured cobalt–tungsten alloys coatings. Trans Inst Met Finish 2016; 94: 313–321.
[23] Rupert TJ, Schuh CA. Sliding wear of nanocrystalline Ni-W: Structural evolution and the apparent breakdown of Archard scaling. Acta Material 2010; 58: 4137–4148.
[24] Sriraman KR, Ganesh Sundara Raman S, Seshadri SK. Corrosion behaviour of

electrodeposited nanocrystalline Ni-W and Ni-Fe-W alloys. Materials Science Engineering A 2007; 460–461: 39–45.

[25] Atanassov N, Gencheva K, Bratoeva M. Properties of Nickel-Tungsten Alloys Electrodeposited from Sulfamate Electrolyte. Plat Surf Finish 1997; 84: 67–71.

[26] Wasekar NP, Hebalkar N, Jyothirmayi A Influence of pulse parameters on the mechanical properties and electrochemical corrosion behavior of electrodeposited Ni-W alloy coatings with high tungsten content. Corrosion Science 2020; 165: 108409.

[27] Sriraman KR, Sundara Raman SG, Seshadri SK. Synthesis and evaluation of hardness and sliding wear resistance of electrodeposited nanocrystalline Ni-W alloys. Materials Science Engineering A 2006; 418: 303–311.